Kinetics of the OH + Methyl Vinyl Ketone and OH + Methacrolein Reactions at Low Pressure

Bao Chuong and Philip S. Stevens*

Environmental Science Research Center, School of Public and Environmental Affairs, Indiana University, Bloomington, Indiana 47405

Received: April 29, 2002; In Final Form: December 6, 2002

The rate constants for the OH + methyl vinyl ketone and OH + methacrolein reactions have been measured in 2−5 Torr of He and over the temperature range 300−422 K using discharge-flow systems coupled with laser-induced fluorescence and resonance fluorescence detection of the OH radical. The rate constant for the OH + methyl vinyl ketone reaction was found to be $(1.73 \pm 0.21) \times 10^{-11}$ cm^3 molecule^{-1} s^{-1} at 5 Torr. No significant pressure dependence was observed between 2 and 5 Torr at 300 K, but a pressure dependence of the rate constant was measured at temperatures between 328 and 422 K. At 328 K, the termolecular rate constant (k_0) was measured to be $(6.71 \pm 2.65) \times 10^{-28}$ cm^6 molecule^{-2} s^{-1}. An Arrhenius expression of $k_0 = (9.9 \pm 7.6) \times 10^{-30} \exp[(1440 \pm 300)/T]$ cm^6 molecule^{-2} s^{-1} over the temperature range 328−422 K was obtained from a weighted linear least-squares fit of the k_0 data versus temperature. Unlike the OH + methyl vinyl ketone reaction, a significant pressure dependence of the rate constant for the OH + methacrolein reaction was not observed between 2 and 5 Torr at $T = 300$−422 K. The measured rate constant was $(3.23 \pm 0.36) \times 10^{-11}$ cm^3 molecule^{-1} s^{-1} at 2 Torr and 300 K, and exhibits a negative temperature dependence over the temperature range 300−422 K.

Introduction

Isoprene (2-methyl-1,3-butadiene) is the most abundant biogenic hydrocarbon emitted into the atmosphere by a variety of plant species with a global source strength exceeding that of anthropogenic nonmethane hydrocarbons.[1,2] Because of its high reactivity, isoprene can significantly contribute to the chemistry of ozone production in the troposphere.[3−6] In addition, two of isoprene's major oxidation byproducts, methyl vinyl ketone (3-buten-2-one) and methacrolein (2-methyl-2-propenal), are also highly reactive and can play an important role in regional ozone production.[6,7]

Methyl vinyl ketone and methacrolein are generated from reactions of isoprene with OH, O_3, and NO_3.[5,6,8−11] Although methyl vinyl ketone can react with O_3 and methacrolein can react with O_3 and NO_3,[11−13] reaction with OH is the dominant process by which both methyl vinyl ketone and methacrolein are removed from the atmosphere.[7,14−16] For the OH + methyl vinyl ketone reaction, OH adds to one of two positions on the double bond in methyl vinyl ketone to form HO−methyl vinyl ketone adducts:[14]

$$OH + CH_3C(O)CH{=}CH_2 + M \rightarrow CH_3C(O)CHCH_2OH + M \quad (1a)$$

$$OH + CH_3C(O)CH{=}CH_2 + M \rightarrow CH_3C(O)CHOHCH_2 + M \quad (1b)$$

Results from product studies suggest that the branching ratio for reaction pathway 1a is at least 70%.[14]

Unlike the OH + methyl vinyl ketone reaction, OH can either add to one of two positions on the double bond in methacrolein or abstract the aldehydic hydrogen:[7,15]

$$OH + CH_2{=}C(CH_3)CHO + M \rightarrow HOCH_2C(CH_3)CHO + M \quad (2a)$$

$$OH + CH_2{=}C(CH_3)CHO + M \rightarrow CH_2C(OH)(CH_3)CHO + M \quad (2b)$$

$$OH + CH_2{=}C(CH_3)CHO \rightarrow CH_2{=}C(CH_3)CO + H_2O \quad (2c)$$

The branching ratio for the OH addition (reactions 2a and 2b) versus the H-atom abstraction mechanism (reaction 2c) has been determined to be 50:50 and 55:45 by Tuazon and Atkinson[15] and Orlando et al.,[7] respectively. Among the addition mechanistic pathways, addition of OH to the terminal carbon (reaction 2a) is believed to be dominant with a branching ratio of at least 85%.[7]

There have been several measurements of the rate constant for the OH + methyl vinyl ketone and the OH + methacrolein reactions, involving both absolute and relative rate studies.[16−21] This paper presents the results of direct measurements of the rate constant for reactions 1 and 2 with M = He at 2−5 Torr and over the temperature range 300−422 K using the discharge-flow technique coupled with laser-induced fluorescence and resonance fluorescence detection of OH. These results are the first reported measurements of the rate constant for these reactions in this pressure range.

Experimental Section

The discharge-flow systems used in this study are similar to those described in detail elsewhere.[22] Briefly, each system consists of a 66-cm-long, 2.5-cm-i.d. Pyrex flow reactor that is

* Corresponding author. E-mail: pstevens@indiana.edu.

10.1021/jp026036q CCC: $25.00
Published on Web 03/07/2003

connected to an aluminum detection chamber. For room-temperature experiments, the interior wall of each flow reactor was coated with a thin film of halocarbon wax (Halocarbon Corporation) to minimize wall losses of reactive species, such as OH. For experiments performed at higher temperatures, a Teflon tube (2.3 cm i.d.) was inserted into the reactor to replace the halocarbon wax, and the flow reactor was wrapped with heating tape to heat it. Temperature was monitored with a thermocouple inserted into the reaction zone of the flow reactor where the carbonyl species is injected. A mechanical pump (Leybold D16B) was used to evacuate each flow reactor system, resulting in a bulk flow velocity of 9.9−14.5 m s^{-1} at 300−422 K. An MKS Baratron capacitance manometer was used to measure the average pressure in the main reaction zone.

OH radicals were produced by either the $F + H_2O \rightarrow OH + HF$ or the $H + NO_2 \rightarrow OH + NO$ reaction. In the first system (S1), F radicals were generated by a microwave discharge of CF_4 (2% in ultrahigh purity (UHP) He, Matheson) through a fixed injector upstream of the main reaction zone. Concentrations of H_2O ($<5 \times 10^{13}$ cm^{-3}) were added 1.3 cm upstream of the F radical injector by bubbling He (Indiana Oxygen, 99.995%) through a trap containing distilled H_2O. In the second system (S2), H radicals were generated by a microwave discharge of trace H_2 (Indiana Oxygen, 99.999%) in He through a fixed injector upstream of the main reaction zone. To promote titration, NO_2 (1.1% in He, Matheson) was added 2 cm upstream of the H radical source, and the NO_2 concentration was determined from the flow rate through a flow controller (MKS 1179).

In S1, laser-induced fluorescence (LIF) was used to detect OH radicals by using the frequency-doubled output of a 20 Hz Nd:YAG-pumped dye laser (Lambda Physik). The excitation of the A−X (1,0) band via the $Q_1(1)$ transition near 282 nm resulted in the OH A−X (0,0) fluorescence near 308 nm. This fluorescence is detected by a photomultiplier tube equipped with photon-counting electronics (Hamamatsu H5920-01) after having passed through a 10-nm band-pass, 20% transmissive interference filter centered at 308 nm (Esco Products).

The detection of OH fluorescence was electronically gated to discriminate against laser light scatter and background fluorescence. The gate was turned on ∼10 ns after the laser pulse, and remained on for ∼300 ns to collect the OH fluorescence. To prevent saturation of the OH absorption and of photon-counting electronics, the average laser power was kept <0.5 mW. At 0.4 mW, the sensitivity of the detection system was $\sim 1 \times 10^{-8}$ counts s^{-1} cm^3 $molecule^{-1}$, calibrated using the $H + NO_2 \rightarrow OH + NO$ reaction. With a typical background signal of 50−100 counts s^{-1}, the OH detection limit was determined to be $\sim 3 \times 10^8$ molecules cm^{-3} (signal-to-noise ratio (S/N) = 1, 10-s integration).

In S2, resonance fluorescence was used to detect OH radicals by using the $A^2\Sigma(v=0) \rightarrow X^2\Pi(v=0)$ transition at 309 nm. The resonance lamp is composed of a flowing mixture of trace distilled H_2O in He excited by a microwave discharge. Radiation from the lamp was collimated by a set of blackened baffles and passed through a quartz window before entering the aluminum detection chamber. To reduce the scatter of lamp radiation inside the detection chamber, light traps were installed opposite the photomultiplier tube and the lamp ports. Photons scattered at a 90° angle to the incident beam exit the detection chamber through another quartz window and are collimated by another set of blackened baffles. These photons were detected by a photomultiplier tube (Hamamatsu H6180-01) equipped with photon-counting electronics after passing through a 10-nm band-pass, 20% transmissive interference filter centered at 308 nm (Esco Products). The sensitivity of the detection system was determined to be $\sim 1 \times 10^{-8}$ counts s^{-1} cm^3 $molecule^{-1}$, calibrated using the $H + NO_2 \rightarrow OH + NO$ reaction. With a typical background signal of ∼500 counts s^{-1}, the detection limit was measured to be $\sim 1 \times 10^9$ molecules cm^{-3} (S/N = 1, 10-s integration).

All experiments were performed under pseudo-first-order kinetic conditions with OH concentrations less than 3×10^{11} molecules cm^{-3}. Concentrations of dilute mixtures of methyl vinyl ketone (Aldrich, 99%) or methacrolein (Aldrich, 95%) were added in excess through a movable 6-mm-o.d. Pyrex injector coated with halocarbon wax. The concentrations were determined from the pressure drop in a calibrated volume over time. Dilute mixtures of methyl vinyl ketone and methacrolein between 1% and 4% were prepared by vacuum-distilling known aliquots of degassed methyl vinyl ketone and methacrolein into the calibrated volume and diluted with UHP He (Indiana Oxygen, 99.999%).

The addition of methyl vinyl ketone and methacrolein increases the loss of OH onto the flow reactor walls, as preliminary pseudo-first-order decays were nonlinear and resulted in large intercepts in the second-order plots. This radical loss is likely a result of the reversible adsorption of the carbonyl species onto the walls of the reactor because the OH signal slowly recovers to its initial value after the flow of the carbonyl species is turned off. This effect has been observed previously in experimental studies of the Cl + isoprene,[23,24] OH + isoprene,[25,26] OH + α-pinene,[27] and OH + β-pinene[27] reactions. Conditioning the flow reactor with high concentrations of F radicals or adding ∼10% O_2 was found to minimize methyl vinyl ketone and methacrolein catalyzed OH wall reactivity, similar to that observed for the OH + isoprene[26] and the OH + α- and β-pinene reactions.[27] It is possible that the fluorine conditioning reduces the polarity of the walls by removing hydrogen atoms from the halocarbon wax coating, while addition of O_2 may inhibit these active sites on the walls. In S1, the flow reactor was conditioned with a large flow of F radicals, and experiments on S1 were performed with and without O_2 added. Instead of conditioning the flow reactor with F radicals in S2, the OH wall reactivity was minimized with the addition of 10% O_2.

Results and Discussion

Pseudo-first-order decay rates (k^I) for the OH + methyl vinyl ketone and OH + methacrolein reactions were calculated from a weighted linear least-squares fit of the logarithm of the OH fluorescence signal versus reaction time, as determined from the distance of the carbonyl injection for reaction under the plug-flow approximation (k^I_{decay}). k^I values were corrected for axial diffusion and OH loss on the movable injector as follows:[28]

$$k^I = k^I_{decay}(1 + k^I_{decay}D/v^2) - k_{probe} \qquad (3)$$

where D is the diffusion coefficient for OH, v is the average bulk gas flow velocity, and k_{probe} is the rate of loss of OH onto the movable injector, measured in the absence of the carbonyl species. The correction for axial diffusion was less than 5%. The effective bimolecular rate constants (k^{II}) at various pressures and temperatures were determined from a weighted linear least-squares fit of k^I values versus carbonyl concentrations. The pressure dependence of k^{II} for reactions 1 and 2 was investigated at five different temperatures in the range 300−422 K.

TABLE 1: OH + Methyl Vinyl Ketone Summary of Experimental Conditions and Results

T (K)	[He] (10^{16} molecules cm^{-3})	[methyl vinyl ketone] (10^{12} molecules cm^{-3})	system used	no. of expts	k^{II} [a] (10^{-11} cm^3 $molecule^{-1}$ s^{-1})
300	6.1	0.6−7.9	S2	22	1.65 ± 0.08
	9.7	0.7−8.3	S2	20	1.63 ± 0.10
	16.1	0.6−12.4	S1, S2	132	1.73 ± 0.04
328	5.6	1.5−17.5	S2	12	0.78 ± 0.08
	9.1	1.5−17.5	S2	13	0.90 ± 0.12
	14.1	0.8−14.4	S1	19	1.22 ± 0.08
361	4.8	1.6−22.0	S2	12	0.58 ± 0.04
	8.0	2.1−23.3	S2	15	0.68 ± 0.02
	13.4	1.6−21.3	S1	21	0.86 ± 0.02
390	4.9	1.9−22.1	S2	12	0.48 ± 0.04
	7.7	1.2−26.0	S2	15	0.59 ± 0.04
	12.4	2.4−24.5	S1	20	0.71 ± 0.04
422	4.3	2.7−22.4	S2	21	0.37 ± 0.02
	7.1	2.0−22.7	S2	22	0.49 ± 0.04
	11.0	1.9−26.3	S1, S2	21	0.56 ± 0.04
flow velocity	9.9−14.5 m s^{-1}				
carrier gas	He; He with 10% O_2				
OH concentration	$<3 \times 10^{11}$ cm^{-3}				
O_2 concentration	$(2-7) \times 10^{15}$ cm^{-3}				
diffusion coefficient	OH in He, $0.145T^{3/2}/P$ (<5% correction)				
first-order wall removal rate	<10 s^{-1}				

[a] Uncertainties represent 2 standard errors.

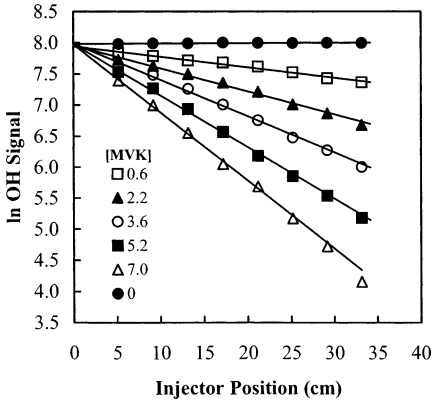

Figure 1. Sample pseudo-first-order decays of OH for the OH + methyl vinyl ketone reaction at 5 Torr and 300 K (methyl vinyl ketone concentrations in 10^{12} cm^{-3}).

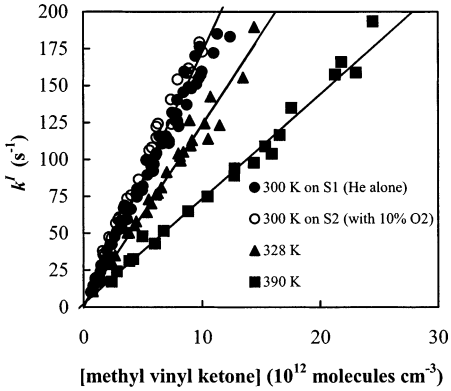

Figure 2. Plot of k^l versus methyl vinyl ketone concentration for the OH + methyl vinyl ketone reaction at 5 Torr and various temperatures.

OH + Methyl Vinyl Ketone. The experimental conditions and the measured rate constants are summarized in Table 1, where the reported uncertainties represent two standard errors from the weighted fit. The data in Table 1 include experiments where different fractions of methyl vinyl ketone/He mixtures were used and the initial OH concentration was varied. The measured rate constants were independent of the fraction of methyl vinyl ketone in the reservoir, suggesting that the heterogeneous loss of methyl vinyl ketone on the uncoated glass wall of the reservoir was minimal.

A series of typical pseudo-first-order OH decay plots for reaction 1 is shown in Figure 1 and the second-order plots for the same reaction measured at 5 Torr and 300, 328, and 390 K appear in Figure 2. As discussed in the above, the measurements of k^l are influenced by methyl vinyl ketone (or methacrolein) catalyzed OH radical loss on the walls of the reactor, as preliminary experiments resulted in nonlinear pseudo-first-order decays of OH and large intercepts in the second-order plots. The conditioning of the flow reactor with high concentrations of fluorine radicals or addition of O_2 improved the linearity of the pseudo-first-order plots and reduced the intercepts on the second-order plots to less than 10 s^{-1} (Figure 2). These intercepts were similar to the first-order wall-loss rates of OH measured in the absence of methyl vinyl ketone or methacrolein, and did not show any correlation with temperature. These results suggest that the conditioning procedure or the addition of O_2 to the flow reactor minimizes heterogeneous effects in these measurements.

A weighted linear least-squares fit of the plot of k^l versus methyl vinyl ketone concentration yields a value of $(1.73 \pm 0.21) \times 10^{-11}$ cm^3 $molecule^{-1}$ s^{-1} for the effective bimolecular rate constant at 300 K and 5 Torr measured in S1 and S2, where the error bar reflects two standard deviations from the weighted fit with an additional 10% to account for systematic errors due to unknown uncertainties in the handling of methyl vinyl ketone.

The measured room temperature rate constant of $(1.73 \pm 0.21) \times 10^{-11}$ cm^3 $molecule^{-1}$ s^{-1} at 5 Torr is in excellent agreement with the rate constant of $(1.79 \pm 0.28) \times 10^{-11}$ cm^3 $molecule^{-1}$ s^{-1} measured by Kleindienst et al.[18] in 50 Torr of argon using a flash photolysis−resonance fluorescence technique, and the relative rate measurements of Cox et al.[17] in 760 Torr of air of 1.69×10^{-11} cm^3 $molecule^{-1}$ s^{-1}at 300 K, normalized to the currently recommended reference molecule rate constant.[16] These results are in reasonable agreement with the results of Gierczak et al.,[16] who measured a rate constant of $(2.03 \pm 0.17) \times 10^{-11}$ cm^3 $molecule^{-1}$ s^{-1} at 298 K in 50−100 Torr of N_2 using a pulsed laser photolysis-pulsed laser induced fluorescence technique. The results reported here are approximately 30% lower than the relative rate measurements

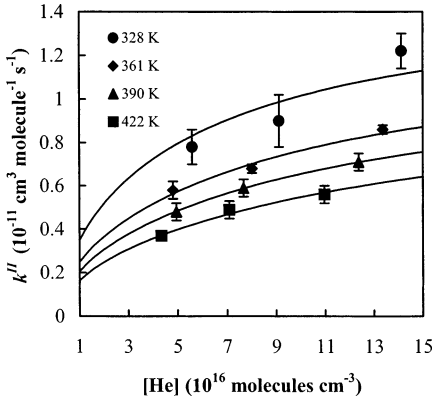

Figure 3. Plot of k^{II} versus [He] at four temperatures in the range 328−422 K for the OH + methyl vinyl ketone reaction. Uncertainties in the data represent 2 standard errors. The solid lines are the weighted least-squares fitting of the falloff behavior using eq 7 and assuming $k_\infty = 4.13 \times 10^{-12} \exp(452/T)$ cm^3 molecule^{-1} s^{-1}.[21]

of Atkinson et al.[19] of $(2.33 \pm 0.18) \times 10^{-11}$ cm^3 molecule^{-1} s^{-1} at 299 K and 1 atm, normalized to the currently recommended reference molecule rate constant.[16]

The agreement between the rate constants measured at low pressures ($(1.65 \pm 0.08) \times 10^{-11}$, $(1.63 \pm 0.10) \times 10^{-11}$, and $(1.73 \pm 0.04) \times 10^{-11}$ cm^3 molecule^{-1} s^{-1} at 2, 3, and 5 Torr, 2σ errors) as reported in this study with those at higher pressures (50 Torr−1 atm) suggests that, at room temperature, reaction 1 is near the high-pressure limit at 2−5 Torr. This suggests that at room temperature the large number of available vibrational degrees of freedom in the HO−methyl vinyl ketone adduct allows the adduct to easily distribute the excess energy resulting from the electrophilic addition of OH to the double bond in methyl vinyl ketone, thereby stabilizing the adduct with a minimal number of third-body collisions. The lack of a significant pressure dependence for reaction 1 at room temperature and between 2−5 Torr and 1 atm is similar to that observed for the OH + isoprene,[25,26] Cl + isoprene,[23,24] OH + α-pinene,[27] OH + β-pinene,[27] and OH reactions with ≥C_4 alkenes.[13]

However, at higher temperatures falloff behavior for reaction 1 is observed for the pressure range 2−5 Torr at temperatures greater than 328 K, as shown in Figure 3, suggesting that the reaction mechanism is dominated by OH addition even at the low pressures and high temperatures of these experiments. These measurements are the first set of direct measurements of the pressure and temperature dependence of this reaction for this pressure range. The observed falloff behavior for reaction 1 is consistent with the following mechanism of the Lindemann−Hinshelwood type:

$$\text{OH} + \text{methyl vinyl ketone} \rightarrow \text{HO−methyl vinyl ketone*} \quad (4)$$

$$\text{HO−methyl vinyl ketone*} \rightarrow \text{OH} + \text{methyl vinyl ketone} \quad (5)$$

$$\text{HO−methyl vinyl ketone*} + \text{M} \rightarrow \text{HO−methyl vinyl ketone} + \text{M*} \quad (6)$$

As the temperature is increased to >328 K, the rate of dissociation of the energized HO−methyl vinyl ketone* complex (reaction 5) begins to compete with the rate of stabilization (reaction 6). A similar effect has been observed for the OH + isoprene reaction.[26]

According to Troe,[29] the effective bimolecular rate constant k^{II} for association reactions along a falloff curve can be represented by

$$k^{II} = \left[\frac{k_0(T)[\text{M}]}{1 + (k_0(T)[\text{M}]/k_\infty(T))}\right] F_c^{(1+[\log(k_0(T)[\text{M}]/k_\infty(T))]^2)^{-1}} \quad (7)$$

where k_0 is the termolecular rate constant at the low-pressure limit, k_∞ is the effective bimolecular rate constant at the high-pressure limit, and F_c is the collision broadening factor at the center of the falloff curve. F_c corrects for the difference between an actual falloff curve and Lindemann−Hinschelwood behavior, which tends to overpredict rate constants in the region near the center of the falloff.[29] This correction increases with increasing number of vibrational modes, increasing strength in the dissociating bond, and increasing temperature.[30]

Given the limited pressure range in this study, both k_0 and k_∞ cannot be accurately calculated. However, if the recommended value for $k_\infty = 4.13 \times 10^{-12} \exp(452/T)$ cm^3 molecule^{-1} s^{-1} and $F_c = 0.6$ are used,[21,31] a weighted nonlinear least-squares fit of the k^{II} data in the temperature range 328−422 K (from Table 1) according to eq 7 would yield the k_0 values listed in Table 2. However, the use of a single value for F_c may not be appropriate for this system, as the data at 328 K are more consistent with $F_c = 0.7$ while the room-temperature measurements near the high-pressure limit are more consistent with Lindemann−Hinschelwood behavior. Additional measurements of the pressure dependence of reaction 1 would be valuable in further characterizing the falloff behavior of this reaction.

Arrhenius parameters were determined by plotting the calculated k_0 values versus temperature, as shown in Figure 4. A weighted linear least-squares fit of the Arrhenius plot yields the following equation for the temperature dependence of the rate constant for reaction 1 at the low-pressure limit with the uncertainties representing two standard errors from the fit:

$$k_0 = (9.9 \pm 7.6) \times 10^{-30} \times \exp[(1440 \pm 300)/T] \text{ cm}^6 \text{ molecule}^{-2} \text{ s}^{-1} \quad (8)$$

TABLE 2: Termolecular Rate Constants Derived fromTroe's Theory for the OH + Methyl Vinyl Ketone Reaction

T (K)	k_0[a] (10^{-28} cm^6 molecule^{-2} s^{-1})
328	6.71 ± 2.65
361	5.17 ± 0.53
390	4.02 ± 0.05
422	2.94 ± 0.19

[a] Uncertainties represent 2 standard errors.

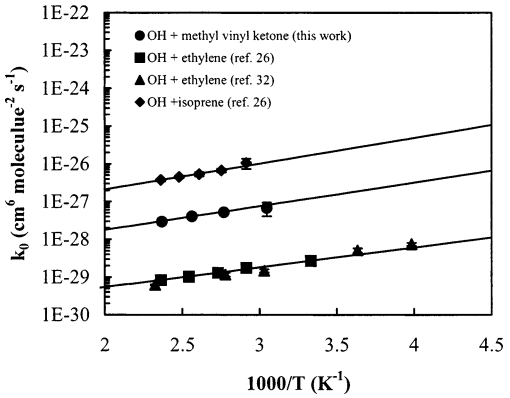

Figure 4. Arrhenius plot of the termolecular rate constants for the OH + methyl vinyl ketone, ethylene, and isoprene reactions. Uncertainties in the data represent 2 standard errors.

TABLE 3: OH + Methacrolein Summary of Experimental Conditions and Results

T (K)	[He] (10^{16} molecules cm^{-3})	[methacrolein] (10^{12} molecules cm^{-3})	system used	no. of expts	k^{II} [a] (10^{11} cm^3 molecule^{-1} s^{-1})
300	6.4	0.4−6.2	S2	25	3.24 ± 0.18
	9.7	0.6−5.9	S2	30	3.22 ± 0.14
	16.1	0.4−6.3	S1, S2	139	3.23 ± 0.04
328	5.6	1.8−9.2	S2	10	2.01 ± 0.32
	8.8	1.3−9.0	S2	10	2.08 ± 0.10
	15.0	1.2−7.9	S1	20	2.19 ± 0.08
361	5.3	0.6−10.5	S2	25	1.82 ± 0.10
	8.0	1.1−11.1	S2	23	1.86 ± 0.08
	13.9	1.3−9.5	S1	30	1.90 ± 0.08
390	4.9	0.9−11.5	S2	13	1.36 ± 0.04
	7.7	0.9−10.6	S2	13	1.46 ± 0.04
	12.4	1.7−10.7	S1	20	1.42 ± 0.06
422	4.6	1.1−14.9	S2	21	1.16 ± 0.04
	6.9	0.8−13.6	S2	21	1.18 ± 0.08
	11.4	1.8−13.2	S1, S2	20	1.18 ± 0.06

flow velocity	10.1−14.5 m s^{-1}
carrier gas	He; He with 10% O_2
OH concentration	$<3 \times 10^{11}$ cm^{-3}
O_2 concentration	$(2-7) \times 10^{15}$ cm^{-3}
diffusion coefficient	OH in He, $0.145T^{3/2}/P$ (<5% correction)
first-order wall removal rate	<10 s^{-1}

[a] Uncertainties represent 2 standard errors.

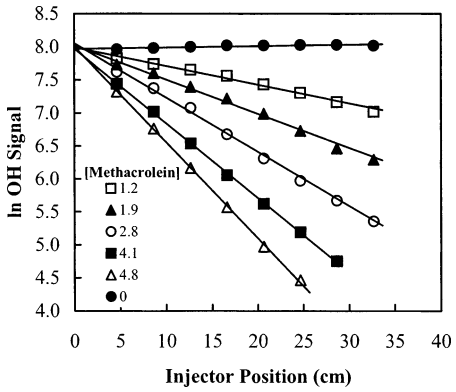

Figure 5. Sample pseudo-first-order decays of OH for the OH + methacrolein reaction at 5 Torr and 300 K (methacrolein concentrations in 10^{12} cm^{-3}).

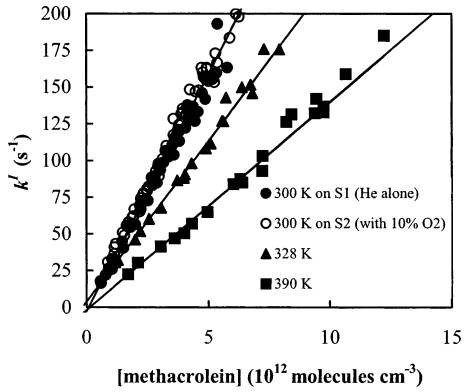

Figure 6. Plot of k^I versus methacrolein concentration for the OH + methacrolein reaction at 5 Torr and various temperatures.

This large negative activation energy of the low-pressure limiting rate constant is similar to those observed for the OH + ethylene[26,32] and OH + isoprene[26] reactions as shown in Figure 4, and is consistent with an OH addition mechanism.

OH + Methacrolein. Table 3 summarizes the conditions of the experiments and the measured rate constants for reaction 2, where the uncertainties represent two standard errors from the weighted fit. Similar to experiments for the OH + methyl vinyl ketone reaction, Table 3 includes experiments where different initial OH concentrations and different fractions of methacrolein/He mixtures were used. Because the measured rate constants were independent of the fraction of methacrolein in the reservoir, it is likely that heterogeneous loss of methacrolein on the walls of the glass reservoir was negligible.

Typical pseudo-first-order decays of OH are shown in Figure 5, and typical plots of k^I versus methacrolein concentration at 5 Torr and 300, 328, and 390 K appear in Figure 6. A weighted least-squares fit of the 300 K second-order plot yields a value of $k^{II}_{300} = (3.23 \pm 0.36) \times 10^{-11}$ cm^3 molecule^{-1} s^{-1} for the effective bimolecular rate constant at 5 Torr, where the error bar reflects two standard deviations from the weighted fit with an additional 10% to account for systematic errors due to unknown uncertainties in the handling of methacrolein.

These room-temperature results are in excellent agreement with the rate constant of $(3.14 \pm 0.49) \times 10^{-11}$ cm^3 molecule^{-1} s^{-1} measured by Kleindienst et al.[18] in 50 Torr of argon using a flash photolysis−resonance fluorescence technique. They also agree well with the relative rate measurements at 1 atm by Atkinson et al.[19] of $(3.52 \pm 0.28) \times 10^{-11}$ cm^3 molecule^{-1} s^{-1} at 299 K, normalized to the currently recommended reference molecule rate constant.[16] The results reported here are also in reasonable agreement with the measurements of Gierczak et al., who measured a rate constant of $(2.79 \pm 0.12) \times 10^{-11}$ cm^3 molecule^{-1} s^{-1} at 298 K using a pulsed laser photolysis−pulsed laser induced fluorescence technique in 20−300 Torr of He and N_2.[16] These results are approximately 30% lower than the relative rate value measured by Edney et al.[20] of $(4.43 \pm 0.35) \times 10^{-11}$ cm^3 molecule^{-1} s^{-1} at 298 K, normalized to the currently recommended reference molecule rate constant.[16]

No significant pressure dependence was observed for reaction 2 at room temperature between 2 and 5 Torr [$(3.24 \pm 0.18) \times 10^{-11}$, $(3.22 \pm 0.14) \times 10^{-11}$, and $(3.23 \pm 0.04) \times 10^{-11}$ cm^3 molecule^{-1} s^{-1} at 2, 3, and 5 Torr, respectively, 2σ errors], similar to that observed at room temperature for reaction 1. These data are the first direct measurements of the rate constant for this reaction in this pressure range. The agreement between the room-temperature results reported here with those at higher pressures (where the OH addition channel is at the high-pressure

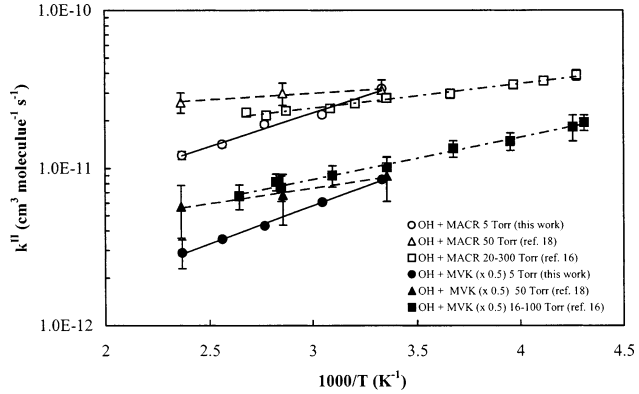

Figure 7. Temperature dependence of the effective bimolecular rate constants for the OH + methacrolein reaction at 5, 50, and 20−300 Torr, and the OH + methyl vinyl ketone reaction at 5, 50, and 16−100 Torr. The rate constants for the OH + methyl vinyl ketone reaction have been reduced by a factor of 2 for clarity.

limit)[16] suggests that, at room temperature, the large number of vibrational degrees of freedom in the HO−methacrolein adducts produced in reactions 2a and 2b allows the adducts to easily distribute the excess energy resulting from the addition of OH to the C−C double bond in methacrolein, thereby stabilizing the adducts with a minimal number of third-body collisions.

Similar to the OH + methyl vinyl ketone reaction, one might expect that the OH + methacrolein addition channels (reactions 2a and 2b) would exhibit a pressure dependence with increasing temperature, as the rate of dissociation of the OH−methacrolein adduct may begin to compete with the rate of stabilization. However, significant falloff behavior at higher temperatures was not observed for this reaction between 2 and 5 Torr. These results may suggest that the H-atom abstraction channel is dominating the overall rate constant at higher temperatures as the contribution of the pressure-dependent OH addition channel decreases, leading to a weak pressure dependence of the overall rate constant for this reaction that may be within the uncertainty of these measurements. Additional measurements over a larger pressure range would be useful in fully characterizing the falloff behavior for this reaction.

Figure 7 shows a plot of the effective bimolecular rate constant versus temperature at 5 Torr for reaction 2. A weighted least-squares fit of the data yields a value of $k = (9.8 \pm 3.8) \times 10^{-13}$ exp[$(1050 \pm 120)/T$] cm^3 molecule^{-1} s^{-1} for the temperature dependence of reaction 2 at 5 Torr between 300 and 422 K, where the uncertainty is two standard deviations from the weighted fit. This observed negative temperature dependence for the OH + methacrolein reaction at 5 Torr is greater than that measured by Kleindienst et al. at 50 Torr between 300 and 423 K ($k = 1.77 \times 10^{-11}$ exp[$(175 \pm 52)/T$] cm^3 molecule^{-1} s^{-1})[18] and the measurements of Gierczak et al. at 20−100 Torr between 234 and 373 K ($k = (7.73 \pm 0.65) \times 10^{-12}$ exp[$(379 \pm 46)/T$] cm^3 molecule^{-1} s^{-1})[16] (Figure 7), but is similar to that observed at 5−6 Torr for the OH + ethylene,[26,32] OH + isoprene,[26] OH + α-pinene,[27] and OH + β-pinene reactions[27] as well as the 5 Torr results for the OH + methyl vinyl ketone reaction presented here. A weighted least-squares fit of the 5 Torr data for the OH + methyl vinyl ketone data in Table 1 yields a value of $k = (3.4 \pm 0.8) \times 10^{-13}$ exp[$(1170 \pm 80)/T$] cm^3 molecule^{-1} s^{-1} for the temperature dependence of reaction 1 at 5 Torr, where the error is two standard deviations from the weighted fit. This observed negative temperature dependence for the OH + methyl vinyl ketone reaction at 5 Torr is also greater than that measured by Kleindienst et al. at 50 Torr between 298 and 424 K ($k = 3.85 \times 10^{-12}$ exp[$(456 \pm 73)/T$] cm^3 molecule^{-1} s^{-1})[18] and the measurements of Gierczak et al. at 16−100 Torr and between 232 and 378 K ($k = (2.67 \pm 0.45) \times 10^{-12}$ exp[$(612 \pm 49)/T$] cm^3 molecule^{-1} s^{-1})[16] (Figure 7).

The large negative temperature dependence at 5 Torr for both reactions 1 and 2 observed in this study compared to the observed negative temperature dependence at higher pressures (Figure 7) is likely due to the fact that the rate constants for both the OH + methacrolein and OH + methyl vinyl ketone reactions are in the low-pressure falloff region for the OH addition channels under the conditions of these experiments. As the temperature increases, the rate of dissociation of the excited OH adducts produced in reactions 1 and 2 begins to compete with the rate of stabilization, resulting in lower observed rate constants at lower pressures than that observed at higher pressures, resulting in a larger observed negative temperature dependence at low pressure (Figure 7). The observed pressure dependence for the OH + methyl vinyl ketone reaction at higher temperatures supports this conclusion. However, as noted above, significant falloff behavior at higher temperatures was not observed for the OH + methacrolein reaction between 2 and 5 Torr. As discussed above, these results may suggest that the H-atom abstraction channel (reaction 2c) is dominating the overall rate constant at higher temperatures, resulting in a weaker pressure dependence of the overall rate constant for reaction 2 compared to reaction 1 that may be within the uncertainty of these measurements. The observed negative temperature dependence of the OH + methacrolein reaction is similar to that observed for the reaction of OH with aliphatic aldehydes,[21,33,34] and may represent an upper limit to the temperature dependence for the H-atom abstraction channel, as the contribution of the addition channels (reactions 2a and 2b) to the overall rate constant likely decreases with increasing temperature. Additional measurements of the pressure dependence of this reaction over a broader range of pressures and temperatures are needed in order to fully characterized the falloff behavior of this reaction.

Conclusions

The measured rate constants for the OH + methyl vinyl ketone reaction between 2 and 5 Torr of He and at 300 K are in good agreement with previous measurements at higher pressures, suggesting that the reaction is near the high-pressure limit between 2 and 5 Torr. Although the lack of a pressure dependence at room temperature may suggest that an H-atom abstraction mechanism may be occurring under these conditions, the observed pressure dependence at >328 K suggests that the reaction is dominated by an addition mechanism even at the lowest pressures and highest temperatures of these experiments, similar to that observed for the OH + isoprene reaction.[26]

Termolecular rate constants at the low-pressure limit for the OH + methyl vinyl ketone reaction appear to be highly temperature dependent. The large negative activation energy observed at the low-pressure limit is similar to that observed in previous studies of the OH + ethylene[26,32] and OH + isoprene reactions.[26] The data for methyl vinyl ketone are the first set of direct measurements of the pressure and temperature dependence for this pressure range.

The observed negative temperature dependence for the OH + methacrolein reaction at 2−5 Torr is greater than that observed at higher pressures, suggesting that the OH addition channel is in the low-pressure falloff regime under these conditions, similar to the OH + methyl vinyl ketone reaction. However, unlike the OH + methyl vinyl ketone reaction, no significant pressure dependence was observed for the OH +

methacrolein reaction between 2 and 5 Torr and at temperatures between 300 and 422 K. These results suggest that the H-atom abstraction channel is dominating the overall rate constant at higher temperatures.

Because of the limited pressure range in this study, more measurements covering a broader pressure range and over an extended temperature range are needed to fully characterize the falloff behavior of both the OH + methyl vinyl ketone and OH + methacrolein reactions and to obtain a more accurate Arrhenius expression that includes both the OH addition and the H-atom abstraction channels for the OH + methacrolein reaction. Future work will examine these reactions at higher pressures using turbulent flow techniques and will examine the kinetics of some of the subsequent steps in the oxidation mechanism.

Acknowledgment. This work is supported by a grant from the National Science Foundation (ATM-9984152). We also thank two anonymous reviewers for their constructive comments on the manuscript.

References and Notes

(1) Lamb, B.; Guenther, A.; Gay, D.; Westburg, H. *Atmos. Environ.* **1987**, *21*, 1695.

(2) Guenther, A.; Hewitt, C. N.; Erickson, D.; Fall, R.; Geron, C.; Graedel, T.; Harley, P.; Klinger, L.; Lerdau, M.; McKay, W. A.; Pierce, T.; Scholes, B.; Steinbrecher, R.; Tallamraju, R.; Taylor, J.; Zimmerman, P. *J. Geophys. Res.* **1995**, *100*, 8873.

(3) Lloyd, A. C.; Atkinson, R.; Lurmann, F. W.; Nitta, B. *Atmos. Environ.* **1983**, *17*, 1931.

(4) Atkinson, R.; Aschmann, S. M.; Tuazon, E. C.; Arey, J.; Zielinska, B. *Int. J. Chem. Kinet.* **1989**, *21*, 593.

(5) Paulson, S. E.; Flagan, R. C.; Seinfeld, J. H. *Int. J. Chem. Kinet.* **1992**, *24*, 79.

(6) Carter, W. P. L.; Atkinson, R. *Int. J. Chem. Kinet.* **1996**, *28*, 497.

(7) Orlando, J. J.; Tyndall, G. S.; Paulson, S. E. *Geophys. Res. Lett.* **1999**, *26*, 2191.

(8) Tuazon, E. C.; Atkinson, R. *Int. J. Chem. Kinet.* **1990**, *22*, 1221.

(9) Paulson, S. E.; Flagan, R. C.; Seinfeld, J. H. *Int. J. Chem. Kinet.* **1992**, *24*, 103.

(10) Grosjean, D.; Willaims, E. L., II; Grosjean, E. *Environ. Sci. Technol.* **1993**, *27*, 830.

(11) Aschmann, S. M.; Atkinson, R. *Environ. Sci. Technol.* **1994**, *28*, 1539.

(12) Aschmann, S. M.; Arey, J.; Atkinson, R. *Atmos. Environ.* **1996**, *30*, 2939.

(13) Atkinson, R. *J. Phys. Chem. Ref. Data* **1997**, *26*, 215.

(14) Tuazon, E. C.; Atkinson, R. *Int. J. Chem. Kinet.* **1989**, *21*, 1141.

(15) Tuazon, E. C.; Atkinson, R. *Int. J. Chem. Kinet.* **1990**, *22*, 591.

(16) Gierczak, T.; Burkholder, J. B.; Talukdar, R. K.; Mellouki, A.; Barone, S. B.; Ravishankara, A. R. *J. Photochem. Photobiol. A: Chem.* **1997**, *110*, 1.

(17) Cox, R. A.; Derwent, R. G.; Williams, M. R. *Environ. Sci. Technol.* **1980**, *14*, 57.

(18) Kleindienst, T. E.; Harris, G. W.; Pitts, J. N., Jr. *Environ. Sci. Technol.* **1982**, *16*, 844.

(19) Atkinson, R.; Aschmann, S. M.; Pitts, J. N., Jr. *Int. J. Chem. Kinet.* **1983**, *15*, 75.

(20) Edney, E. O.; Kleindienst, T. E.; Corse, E. W. *Int. J. Chem. Kinet.* **1986**, *18*, 1355.

(21) Atkinson, R. *J. Phys. Chem. Ref. Data* **1989**, *18*, Monograph 1, 1.

(22) Loewenstein, L. M.; Anderson, J. G. *J. Phys. Chem.* **1984**, *88*, 6227.

(23) Stutz, J.; Ezell, M. J.; Ezell, A. A.; Finlayson-Pitts, B. J. *J. Phys. Chem. A* **1998**, *102*, 8510.

(24) Bedjanian, Y.; Laverdet, G.; LeBras, G. *J. Phys. Chem. A* **1998**, *102*, 953.

(25) Stevens, P.; L'Esperance, D.; Chuong, B.; Martin, G. *Int. J. Chem. Kinet.* **1999**, *31*, 637.

(26) Chuong, B.; Stevens, P. S. *J. Phys. Chem. A* **2000**, *104*, 5230.

(27) Chuong, B.; Davis, M.; Edwards, M.; Stevens, P. S. *Int. J. Chem. Kinet.* **2002**, *34*, 300.

(28) Howard, C. J. *J. Phys. Chem.* **1979**, *83*, 3.

(29) Troe, J. *J. Phys. Chem.* **1979**, *83*, 114.

(30) Donahue, N. M.; Dubey, M. K.; Anderson, J. G. *J. Geophys. Res.* **1997**, *102*, 6159.

(31) DeMore, W. B.; Sander, S. P.; Golden, D. M.; Hampson, R. F.; Kurylo, M. J.; Howard, C. J.; Ravishankara, A. R.; Kolb, C. E.; Molina, M. J. *Chemical Kinetics and Photochemical Data for Use in Stratospheric Modeling*; NASA JPL Publ. No. 97-4; Jet Propulsion Laboratory: Pasadena, CA, 1997.

(32) Kuo, C.-H.; Lee, Y.-P. *J. Phys. Chem.* **1991**, *95*, 1253.

(33) Atkinson, R. *J. Phys. Chem. Ref. Data* **1994**, *23*, Monograph 2, 1.

(34) Tyndall, G. S.; Staffelbach, T. A.; Orlando, J. J.; Calvert, J. G. *Int. J. Chem. Kinet.* **1995**, *27*, 1009.